

We are IntechOpen, the world's leading publisher of Open Access books Built by scientists, for scientists

5,300

Open access books available

130,000

International authors and editors

155M

Downloads

Our authors are among the

154

Countries delivered to

TOP 1%

most cited scientists

12.2%

Contributors from top 500 universities



WEB OF SCIENCE™

Selection of our books indexed in the Book Citation Index
in Web of Science™ Core Collection (BKCI)

Interested in publishing with us?
Contact book.department@intechopen.com

Numbers displayed above are based on latest data collected.
For more information visit www.intechopen.com



Type-2 Fuzzy Sets based Ego-Motion Compensation of a Humanoid Robot for Object Recognition

Tae-Koo Kang and Gwi-Tae Park
School of Electrical Engineering, Korea University
Korea

1. Introduction

Humanoid robots have the similar appearance to human being with a head, two arms and two legs, and has some intelligent abilities as human being, such as object recognition, tracking, voice identification, obstacle avoidance, and so on. Since they try to simulate the human structure and behavior and they are autonomous systems, most of the times humanoid robots are more complex than other kinds of robots. In the case of moving over an obstacle or detecting and localizing an object, it is critically important to attain as much precise information regarding obstacles/object as possible since the robot establishes contact with an obstacle/object by calculating the appropriate motion trajectories to the obstacle/object. Vision system supplies most of the information, but the image sequence from the vision system of a humanoid robot is not static when a humanoid robot is walking, so some problems occur due to the ego-motion. Therefore, the humanoid robots need the algorithms that can autonomously determine their action and paths in unknown environments and compensate the ego-motion using the vision system. The vision system is one of the most important sensors in the humanoid robot system, it can supply lots of information which a humanoid robot needs. However the vision system indispensably requires the stabilization module, which can compensate the ego-motion of itself for the more precise recognition.

Over the years, a number of researches have been achieved in motion compensation field on the vision system mounted in the robot. Some researches use single camera, but the stereovision, which can extract information regarding the depth of the environment, is commonly used. Robot motion from stereo-vision can be estimated by the 3D rigid transform, using the 2D multi-scale tracker, which projects 3D depth information on the 2D feature space. The scale invariant feature transform (SIFT) (Hu et al., 2007), which is a local feature based algorithms to extract features from images and estimate transformation using their location, and iterative closest point (ICP) (Milella & Siegwart, 2006), which is used for registration of digitized data from a rigid object with an idealized geometric model, have been used mainly for motion estimation using single camera or stereo camera for the video stabilization or autonomous navigation purposes, and have been widely used in wheeled robots (Lienhart & Maydt, 2002)(Beveridge et al., 2001)(Morency & Gupta, 2003). Moreover, the optical flow based method, which can estimate the motion by 3D normal flow constraint using gradient-based error function, is widely used, because of the simplicity of

computation (Vedula et al., 1999). However, these are not appropriate methods for a biped humanoid robot, as walking motions of a humanoid robot simultaneously show the vertical and horizontal movement, unlike the motion of a mobile robot, as well as computation cost yielded by its point to point operation. Therefore, the more efficient stereo-vision based ego-motion estimation method, which is used for the ego-motion compensation, is proposed for a humanoid robot.

The proposed ego-motion compensation method using stereo camera consists of three parts - segmentation, feature extraction, and motion estimation. The stereo vision can obtain disparity images where objects are shown in different gray level according to the different distance between object and the humanoid robot itself. In the segmentation part, objects are extracted by the image analysis using our proposed fuzzy information theoretical approach based on type-2 fuzzy sets. Feature extraction part extracts the feature images using wavelet level set, which can obtain horizontal, vertical and diagonal information for each object. The results of feature extraction part are used as the input data of the estimation part. The position of each object can be calculated using least-square ellipse approximation. The differences of positions between two images are calculated as the compensation parameters. Moreover, a proposed type-2 fuzzy method is used to deal with the noise data to obtain a couple of precise rotation and translation data set.

This paper is organized as follows. In Chapter 2, the proposed the stereo-vision based motion stabilization of a humanoid robot by fuzzy sets is introduced specifically. In Chapter 3, the results of experiments focusing on verifying the performances of the proposed system is given. Chapter 4 concludes the paper by presenting the contributions.

2. Ego-motion compensation system

2.1 Architecture of the proposed ego-motion compensation system

In order to eliminate the error of the object recognition caused by the ego-motion of a humanoid robot when it is walking, we proposed a novel ego-motion compensation system based on fuzzy sets theory using stereo vision information. We also compare the performance using type-1 fuzzy sets and type-2 fuzzy sets, and the results show that the performance using type-2 fuzzy sets is better.

The vision system using SR4000 can supply stereo vision information. The stereo vision is generated based on the perspectives of our two eyes lead to slight relative displacements of objects (disparities) in the two monocular views of scene, then the disparities are used to calculate the distance between the object and the camera in a 3D scene to generate a depth image.

The overall ego-motion compensation system architecture of our proposed method is constructed as illustrated in Fig.1. The system largely consists of three parts: segmentation, feature extraction, and estimation. Finally, the estimation parameters obtained from depth image are used to compensate the ego-motion in gray image for object recognition.

In the segmentation process, the depth image is used as the input image, and the different objects show different depth information which is used to separate objects. Some image processing techniques are needed to preprocess the depth image to get rid of the information irrelative to the objects, such as ground and noise. A new fuzzy sets based segmentation method is proposed, and type-2 fuzzy sets shows better performance than type-1 fuzzy sets. The number of object can be decided automatically, based on the number of local maximum. Then all objects shown in the image are extracted individually.

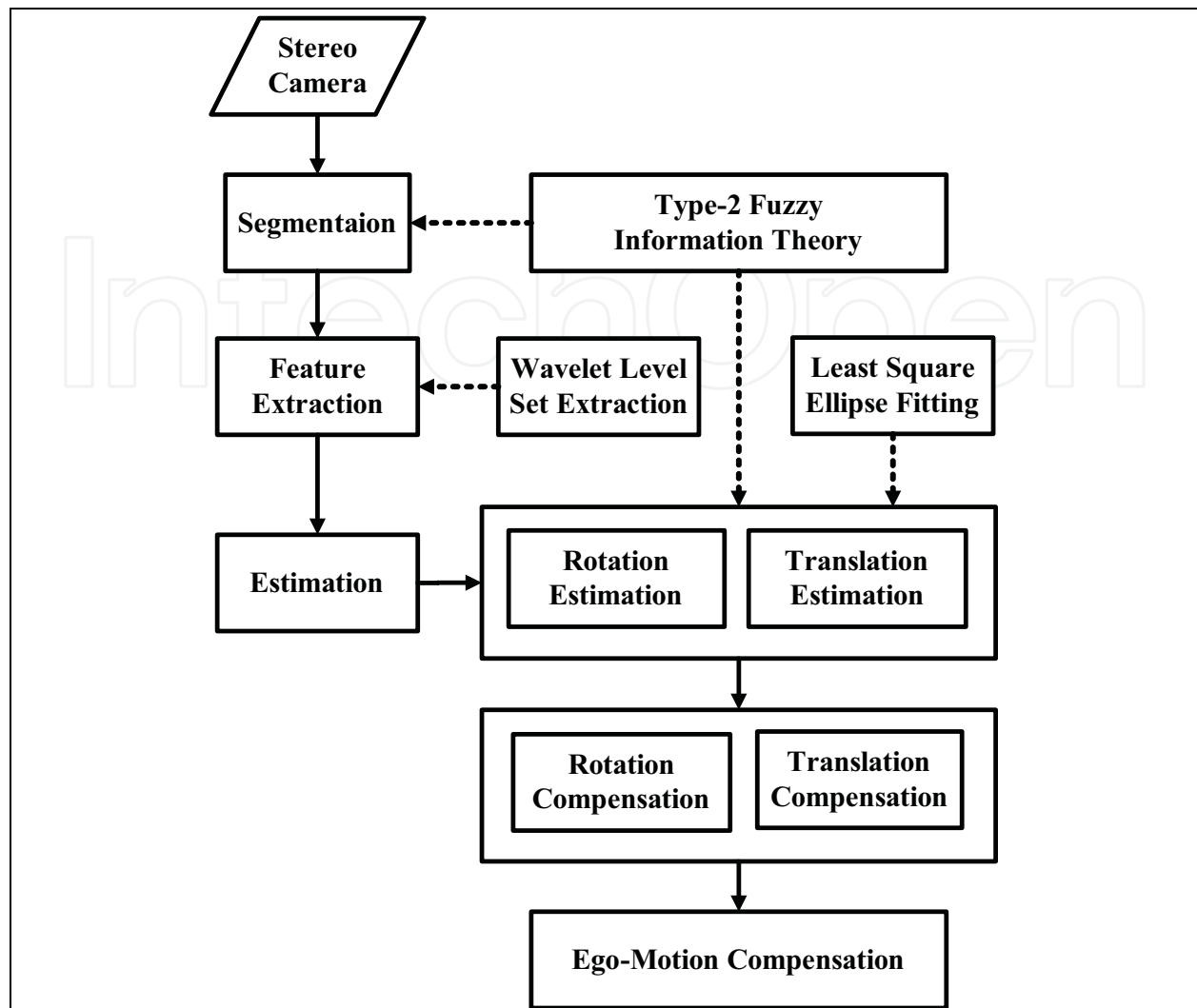


Fig. 1. Overall ego-motion compensation system architecture

In the feature extraction process, the feature data, such as the vertical, horizontal and diagonal coefficients of each segmented object are extracted using wavelet level-set transform.

In the estimation process, the extracted feature data of each object are used to fit an ellipse using the stable least square ellipse fitting method, the center and angle of the ellipse are obtained as the position and angle information of the object, and the difference of ellipse information of the same object in two images are calculated as the displacements for the angle and translation.

Consequently, the average angle and translation displacements of all objects are used as the compensation data in the final compensation process. The detailed explanations are given as follows.

2.2 Disparity image segmentation based on fuzzy information theory

From the depth image, objects can be segmented according to the different gray level. In this thesis, we proposed a novel fuzzy image segmentation method for depth image, which is based on fuzzy sets (Medel, 2001) and fuzzy information theoretical approach. Type-2 fuzzy set based method shows better performance than type-1 based method. The proposed

method is fast and effective. The number of cluster seeds is determined automatically according to the number of local maximum, unlike other clustering method, such as FCM (Hwang & Phee, 2007), which needs to determine it ahead of time.

2.2.1 Fuzzy sets

Fuzzy techniques are suitable for development of new image processing algorithms because as nonlinear knowledge based methods, they are able to remove grayness ambiguities in a robust way.

A type-1 fuzzy set, A , which is in terms of a single variable, $x \in X$, is characterized by a membership function that takes values in the interval $[0, 1]$, and can be defined as .

$$A = \{(x, \mu_A(x)) \mid \forall x \in X\} \quad (1)$$

$\mu_A(x)$: membership function

Type 2 fuzzy sets was introduced first by Zadeh (1975) as an extension of the concept of an ordinary fuzzy set. Type-2 fuzzy sets are high level representation of vague data, and can handle the uncertainties in type-1 fuzzy sets, such as, the meaning of the word and noise measurements.

A type-2 fuzzy set, denoted \tilde{A} , is characterized by a type-2 membership function, $u_{\tilde{A}}(x, u)$, where X is the universal set, $x \in X$ and $u \in J_x \subseteq [0, 1]$. That is,

$$\tilde{A} = \{(x, u), \mu_{\tilde{A}}(x, u) \mid \forall x \in X, \forall u \in J_x \subseteq [0, 1]\} \quad (2)$$

Where $0 \leq u_{\tilde{A}}(x, u) \leq 1$. Accordingly, at each value of x , say $x = x'$,

$$\mu_{\tilde{A}}(x') = \sum_{u \in J_{x'}} f_{x'}(u) / u, \text{ for } u \in J_{x'} \subseteq [0, 1] \text{ and } x' \in X \quad (3)$$

where $u_{\tilde{A}}(x)$ represents the secondary membership function. When $f_x(u) = 1$, $\forall u \in J_x \subseteq [0, 1]$, then the secondary membership functions are interval sets, and, if this is true for $\forall x \in X$, we have the case of an interval type-2 membership function. Interval secondary membership functions reflect a uniform uncertainty at the primary memberships of x .

Uncertainty in the primary memberships of a type-2 fuzzy set, \tilde{A} , consists of a bounded region that is called the footprint of uncertainty (FOU). It is the union of all primary memberships, i.e.,

$$FOU(\tilde{A}) = \bigcup_{X \in x} J_x \quad (4)$$

The FOU can be described in terms of upper and lower membership functions, denoted as $\bar{u}_{\tilde{A}}(x)$ and $\underline{u}_{\tilde{A}}(x)$, which are two type-1 membership functions that are bounds for the FOU of a type-2 fuzzy set. So a type-2 fuzzy set can also be given as follows:

$$\tilde{A} = \{(x, \underline{\mu}_{\tilde{A}}(x), \bar{\mu}_{\tilde{A}}(x)) \mid \forall x \in X, \underline{\mu}_{\tilde{A}}(x) \leq \mu(x) \leq \bar{\mu}_{\tilde{A}}(x) u \in [0, 1]\} \quad (5)$$

The lower and upper membership can be defined by means of linguistic hedges like dilation and concentration:

$$\begin{cases} \underline{\mu}_{\tilde{A}}(x) = [\mu(x)]^\alpha \\ \bar{\mu}_{\tilde{A}}(x) = [\mu(x)]^{1/\alpha} \end{cases} \quad (6)$$

where $\alpha \in (1, \infty)$. Fig.2 shows an example of type 1 fuzzy set and FOU of type 2 fuzzy set for Gaussian primary membership function with uncertain mean. The uniform shading for the FOU denotes interval sets for the secondary membership functions and represents the entire interval type-2 fuzzy set.

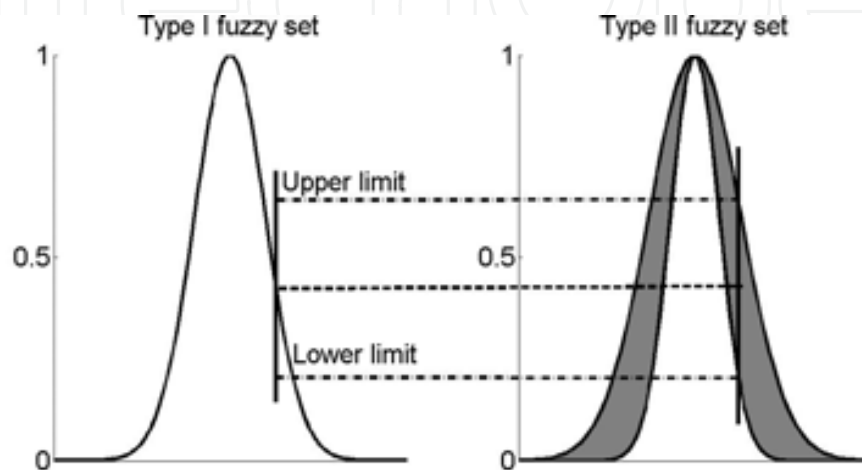


Fig. 2. Example of type-1 and type-2 membership functions.

2.2.2 Information-theoretical approach

Information-theoretical approach is the most used fuzzy technique because of its simplicity and high speed.

This approach minimizes or maximizes measures of fuzziness and image information such as index of fuzziness or crispness, fuzzy entropy, fuzzy divergence, etc. The most common measure of image fuzziness is the linear index of fuzziness. Tizhoosh (Tizhoosh, 2005) (Tizhoosh, 2008) has defined a linear index measure of fuzziness as follows.

$$Fuzziness: \gamma(\tilde{A}) = \frac{2}{MN} \sum_{g=0}^{L-1} h(g) \times \min[\mu_A(g), 1 - \mu_A(g)] \quad (7)$$

where A is an $M \times N$ image subset, and $A \subseteq X$ with L gray levels $g \in [0, L-1]$, $h(g)$ stands for the histogram, $u_A(g)$ stands for the membership function. Here fuzziness is calculated using type-1 fuzzy set $u_A(g)$.

Ultrafuzziness is an extension of fuzziness using type-2 fuzzy set.

$$Ultrafuzziness: \tilde{\gamma}(\tilde{A}) = \frac{2}{MN} \sum_{g=0}^{L-1} h(g) \times [\bar{\mu}_{\tilde{A}}(g) - \underline{\mu}_{\tilde{A}}(g)] \quad (8)$$

$\bar{u}_{\tilde{A}}(g)$ and $\underline{u}_{\tilde{A}}(g)$ stand for the upper and lower membership functions, which are calculated according to (6). Ultrafuzziness can not only remove the vagueness/imprecision in the data but also the uncertainty in assigning membership values to the data.

Tizhoosh (Tizhoosh, 1998) defined the suitable LR-type fuzzy number (9) for image thresholding, which is also suitable for segmentation, as shown in Fig.3, and the type-2 fuzzy membership function is generated using (6).

$$u(g) = \begin{cases} 0, & g \leq g_{\min} \text{ or } g \geq g_{\max}, \\ L(g) = \left(\frac{g - g_{\min}}{T - g_{\min}}\right)^\alpha, & g_{\min} \leq g \leq T, \\ R(g) = \left(\frac{g_{\max} - g}{g_{\max} - T}\right)^\beta, & T \leq g \leq g_{\max} \end{cases} \quad (9)$$

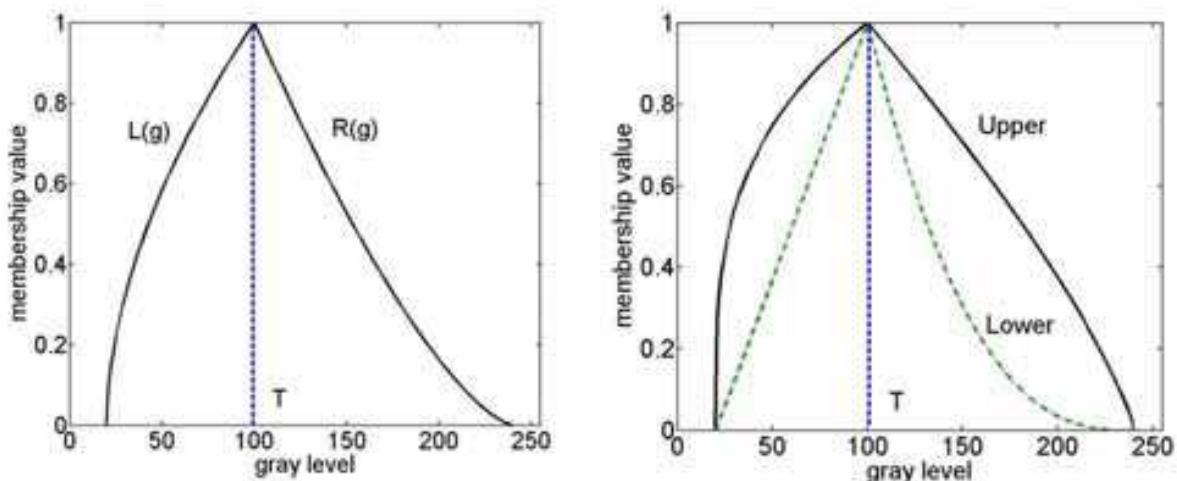


Fig. 3. LR type membership function. Left : type-1 LR type MF right : type-2 LR type MF

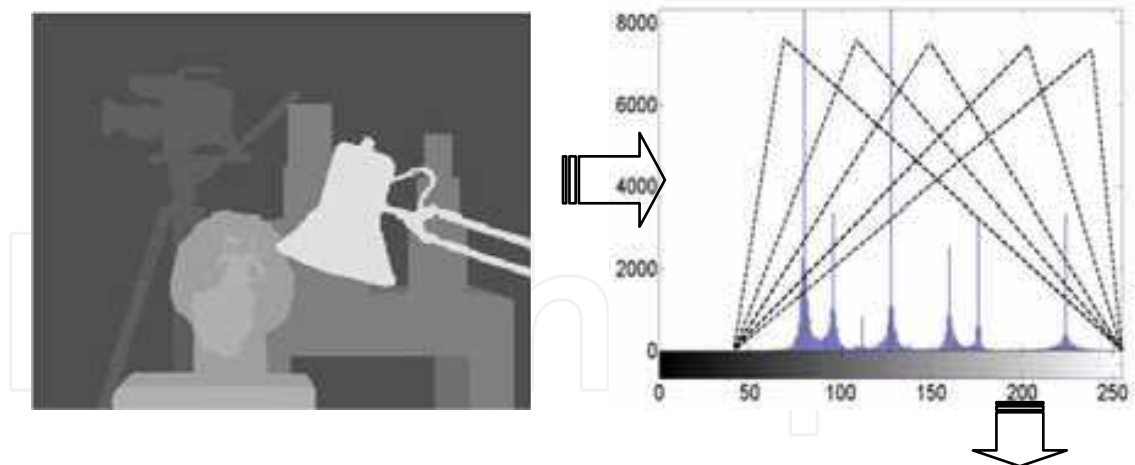
2.2.3 Segmentation algorithm

The general algorithm for our proposed image segmentation method based on type-2 fuzzy sets and fuzzy information theory can be summarized as following,

1. Use the LR shape membership function and initialize α .
2. Calculate the histogram of depth image.
3. Initialize the position of the membership function with minimum and maximum gray level of depth image.
4. Shift the membership function T along the gray-level range in histogram and calculate the amount of ultrafuzziness in each position (e.q. (8)).
5. Locate the segmentation point with local maximum ultrafuzziness.
6. Segment the image with all the segmentation points.

The segmentation algorithm based on type-1 fuzzy sets is almost the same with the algorithm based on type-2 fuzzy sets, except the calculation of fuzziness instead of ultrafuzziness and without initialization of α .

Fig.4 shows an example of the main segmentation process using type-2 fuzzy sets and fuzzy information theory. The begin and end point of gray level range are not considered as local maximum of ultrafuzziness, as shows in Fig.8, the local maximum are shown in red points.



Segment with Local Maximum Calculation of Ultrafuzziness

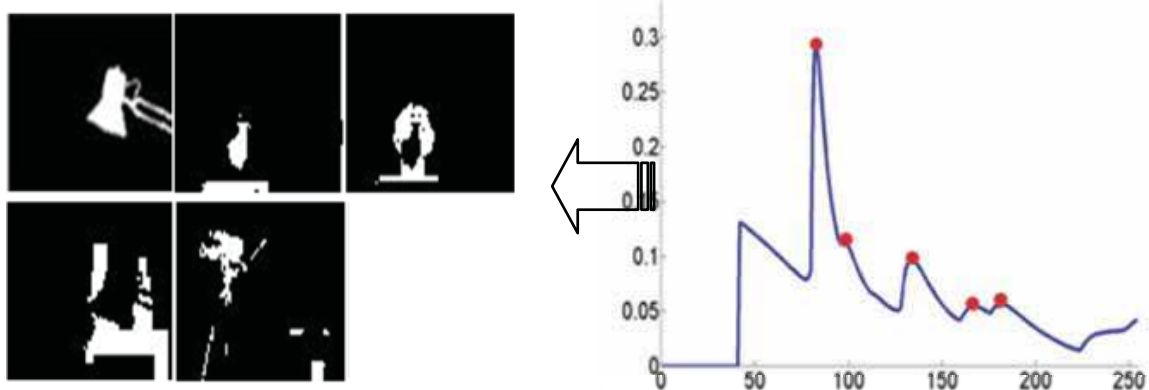


Fig. 4. Proposed segmentation process.

2.2.4 Comparison of type-1 and type-2 fuzzy sets

Fig.5 shows the different segmentation result using type-1 and type-2 fuzzy sets. The calculation results of fuzziness and ultrafuzziness are also showed. There are two local maximum points in fuzziness and five local maximum points in ultrafuzziness. So, only two objects are extracted using type-1 fuzzy sets, and 5 objects are extracted using type-2 fuzzy sets with the last part as the background, which has low gray level.

The difference of the results shows that type-2 fuzzy sets can handle the membership uncertainty and grayness difference to achieve a better segmentation performance than type-1 fuzzy sets. So, the type-2 fuzzy sets based method is proposed for segmentation in this thesis.

2.3 Feature extraction using wavelet transform

Wavelet transforms (Mallat, 1999) in two dimensions are multi-resolution decompositions that can be used to analyze images. The two dimensional DWT can be implemented using digital filters and down-samplers with separable two dimensional scaling and wavelet functions, which are one dimensional DWT of the rows and columns.

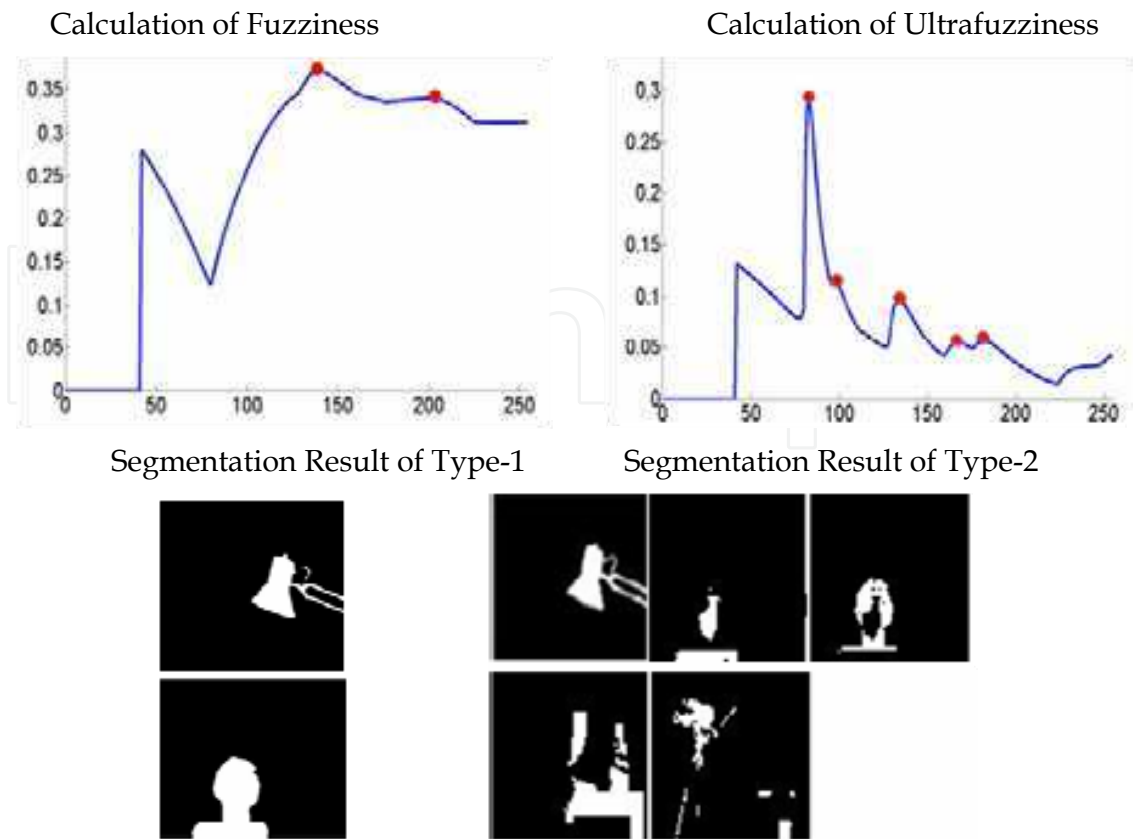


Fig. 5. Comparison of segmentation results based on type-1 and type-2 fuzzy sets.

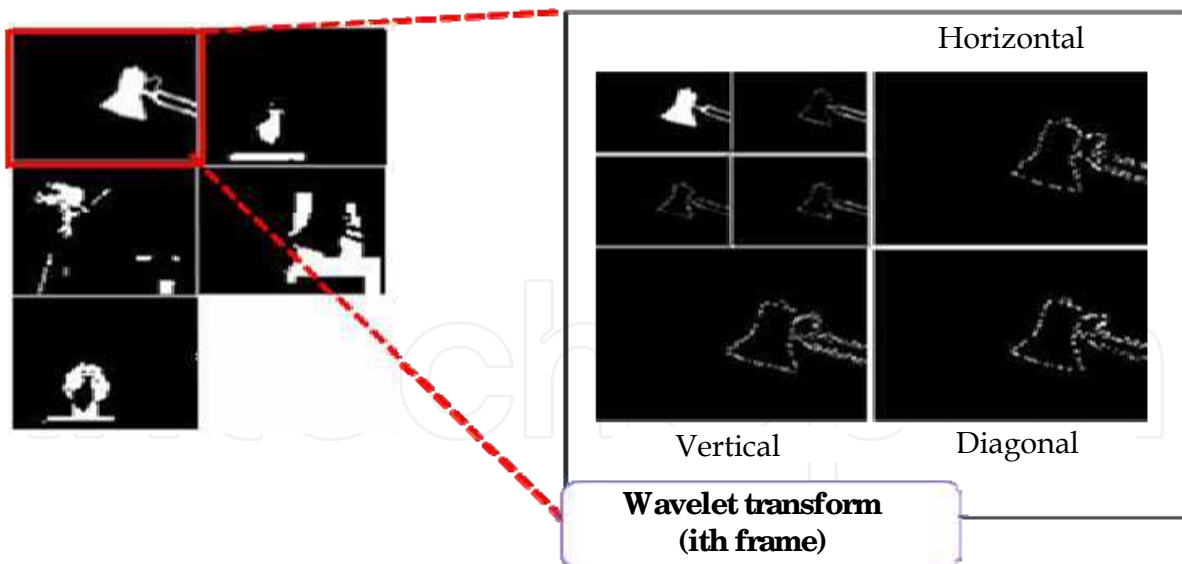


Fig. 6. Level-2 wavelet transform.

The single scale filter bank can be “iterated” to produce a P scale transform. After images are decomposed first, approximation components and detail coefficients (horizontal, vertical and diagonal coefficients) of the first level can be obtained. Then, decomposing directly the approximation components (by tying the approximation output to the input of another filter bank) to obtain approximation components and detail coefficients of the second level.

Repeatedly, multi-level detail coefficients can be found. As shown in Fig.6, the H, V, and D features of the lamp, which is one of the objects segmented, are obtained using level 2 wavelet transform method.

2.4 Rotation and translation estimation

A numerically stable least squares method fitting an ellipse (Radim & Jan, 1998) to a set of data points is proposed to calculate the rotation angle between the image sequences. This method is a simple, stable and robust non-iterative algorithm for fitting an ellipse to a set of data points. It is based on a least squares minimization and it guarantees an ellipse-specific solution even for scattered or noisy data.

This fitting method is robust for the localization of the optimal ellipse solution. The data sets which are used for fitting an ellipse are generated from the wavelet feature extraction process, such as the H, V, and D features. Every data set, the coordinate of the pixels of wavelet decomposed images, belongs to one ellipse, because it stands for one segmented object. The angles and centers of two ellipses from two sequences can be calculated, then the difference of rotation angle and the x, y axis transformation of centers between two sequences can be calculated. The center difference is not the real transformation data, before calculating the transformation $T(x_i, y_i)$, rotation angle should be compensated, and this can be done by a rotation matrix as follow, the center coordinates of ellipses in posterior sequence (C_{i+1}) are rotated around the image center (C_0) and then calculate the difference between the prior sequence (C_i).

$$R_\theta = \begin{pmatrix} \cos(\theta) & -\sin(\theta) \\ \sin(\theta) & \cos(\theta) \end{pmatrix} \quad (15)$$

$$T(x_i, y_i) = R_\theta(C_{i+1} - C_0) - (C_i - C_0)$$

Many rotation and translation values can be obtained according to the level of wavelet transform and the number n of objects segmented ($3 \times \text{level} \times n$), including some big noise values that can occur in the case that the object partially disappears in the sequence image. A type-2 fuzzy threshold method based on fuzzy information theory measures is used to get rid of such noise values. This method, which is similar with our segmentation method, selects two local maximum ultrafuzziness as the optimal threshold to get rid of the left and right noise value, and then the average value can be calculated as the rotation or transformation values.

Finally, the estimated rotation and transformation information are used for ego-motion compensation in image sequence.

Fig.7 shows an example of rotation estimation and compensation, includes wavelet feature extraction, ellipse fitting, noise data deletion to get valid value, estimation and compensation.

3. Experimental results

The performance of the proposed motion compensation method of a humanoid robot is evaluated via experiments. Our experiments can be divided into two sub-experiments, one is estimation performance evaluation, and the other is processing time evaluation. The experiments are proceeded using UR1A, SR4000 camera, and a computer with an AMD 2.3GHz CPU, 2.0GB RAM, and Matlab2008a.

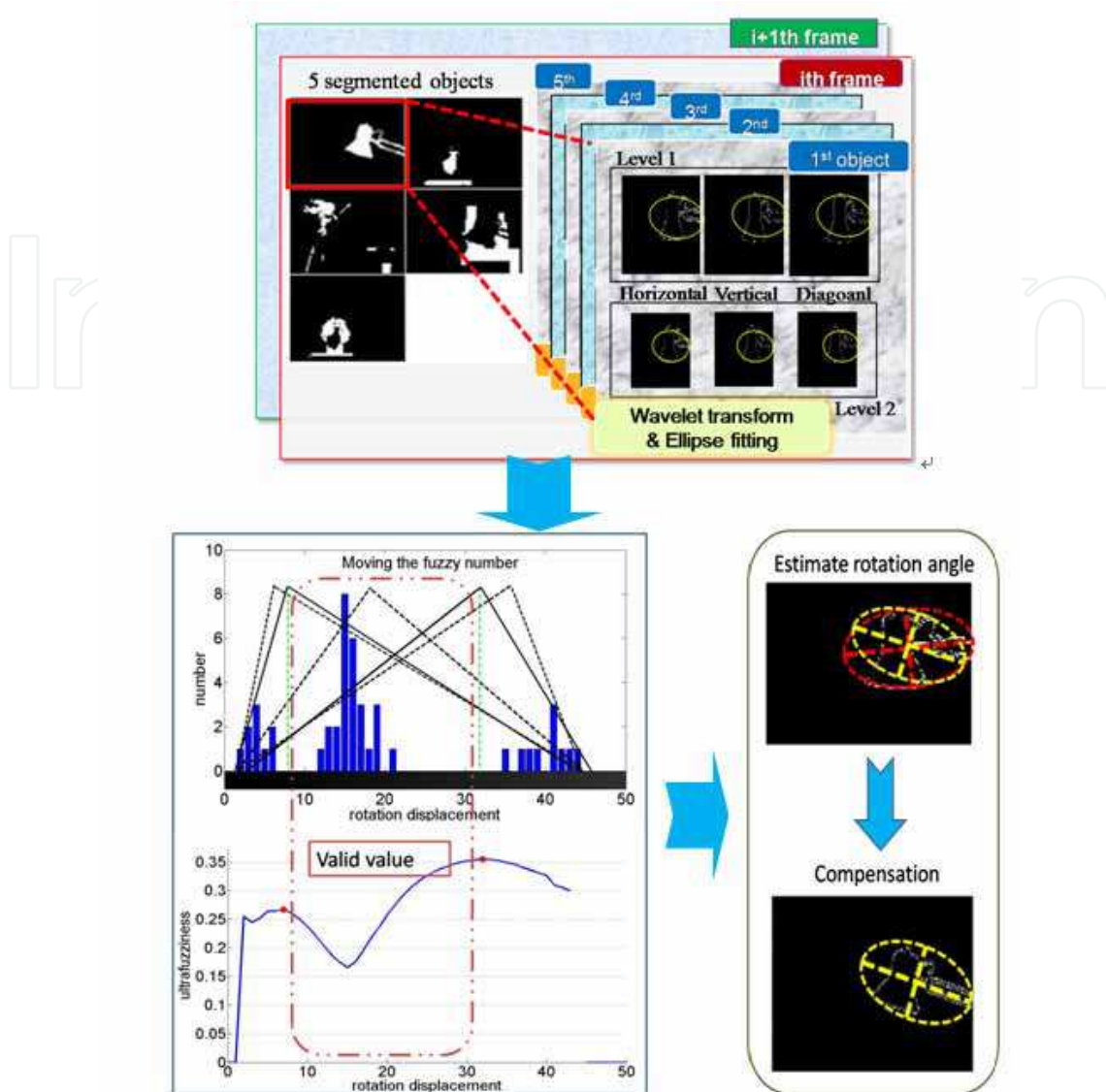


Fig. 7. Level-2 Example of rotation compensation.

3.1 Evaluation of the estimation performance

The proposed method regarding the motion stabilization is evaluated under the artificial ideal environment first. As such, the quantity of errors was determined by comparing the results of the test algorithms with the ideal data. The test algorithms, which are compared with the proposed method for the translation displacement and the rotation displacement, consist of SIFT, ICP. Performance evaluation measures the displacements of x axis, y axis, rotation angle and average error from the ideal case to results of each algorithm for one cycle respectively.

A standard set of stereo pairs with available ground truth (Scharstein, 2002) is used. Each depth values have 256 gray levels with brighter levels representing points closer to the camera and unmatched points depicted as white.

The results of estimation performance evaluation are presented in Fig.8. The origin of coordinate in Fig.8 is the center of the image. The left images in Fig.8 show the estimation performance and the right images in Fig.8 show the errors from the ideal case.

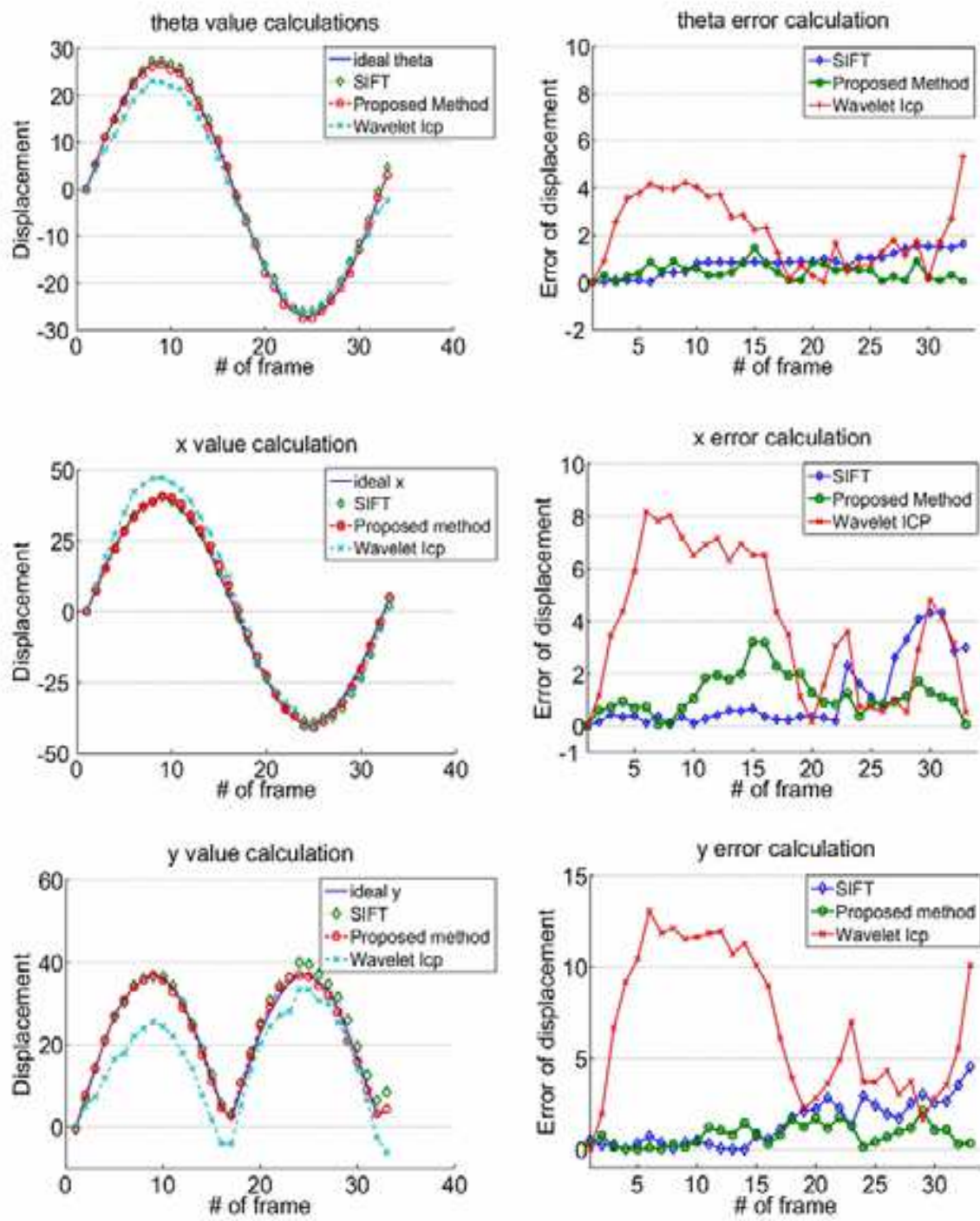


Fig. 8. Results of estimation performance.

Specific results for errors are shown in Table 1. As shown in table 1, proposed method demonstrates a better performance compared to the other algorithms. Especially, the proposed method shows good performance on same plane as SIFT or shows slightly better performance.

Method	Variable	Mean of Errors	Variance
Proposed Method	Rotation error	0.45	0.33
	X-axis error	1.18	0.79
	Y-axis error	0.79	0.59
SIFT	Rotation error	0.83	0.48
	X-axis error	1.12	0.37
	Y-axis error	1.40	1.23
ICP	Rotation error	2.14	1.52
	X-axis error	3.92	2.73
	Y-axis error	6.84	3.96

Table 1. Evaluation results of the estimation performance

3.2 Evaluation of the processing time

The second experiment is the processing time evaluation. The image sequence, which is made from a standard set of stereo pairs with available ground truth, is used. Each image sequence consists of 30, 35 frames and the test is performed 5 times per image sequence. The processing time was measured using the MATLAB and was compared with SIFT and ICP. Table.2 shows the experimental results regarding processing time. The proposed method is faster than the others.

Method	Processing Time(ms)		
	Minimum	Maximum	Average
Propose Method	151	160	156
SIFT	363	381	370
ICP	1472	1525	1490

Table 2. Evaluation results of the processing time

3.3 Evaluation of the processing time

We test the algorithms under the real image sequence obtained from SR4000 camera mounted on the humanoid robot UR1A. Fig.9 shows the ego-motion estimation results which are executed in the real environment. In the Fig.9, X-axis displacements show the peak points around 40 and -40 and Y-axis show the peak points around 32 and 2. Rotation displacement shows the peak point around 12 and -12. Fig.10 shows the image sequence after ego-motion compensation. There are two steps in the compensation process, first is the rotation compensation and the second is transformation compensation.

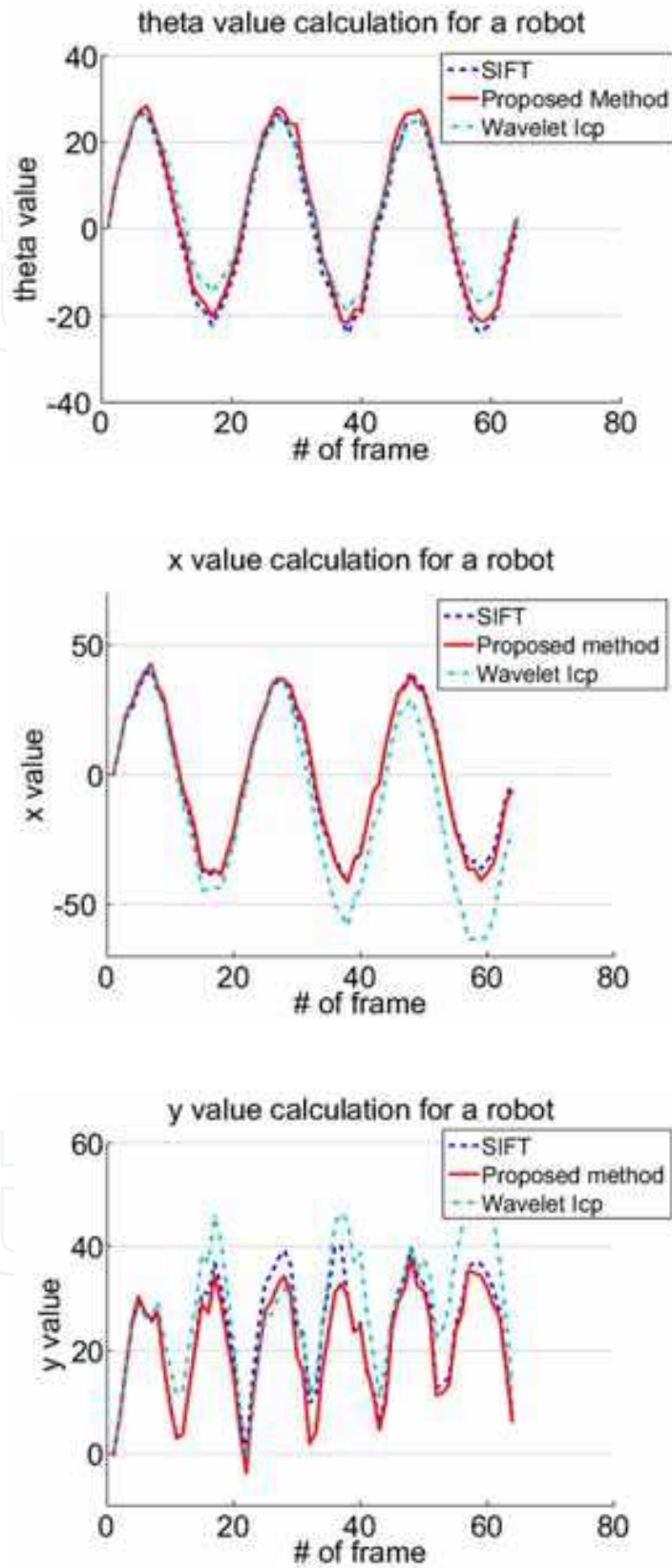


Fig. 9. Motion estimation results for a humanoid robot



Fig. 10. Image sequence after ego-motion compensation

3.4 Object recognition experiments

3.4.1 Training for HMAX model

The training process of object recognition experiments are performed over a set of classes provided by Caltech101 (Caltech, 2003). CalTech101 database contains 101 object classes plus a background class collected by Fei-Fei. These datasets contain the target object embedded in a large amount of clutter in real environment. There are about 40 to 800 images per category and most categories have more than 50 images.

Some object categories and the background example images in the training process as shown in Fig. 11. For each object category, the system was trained with 50 positive examples from the target object class and 50 negative examples from the background class.

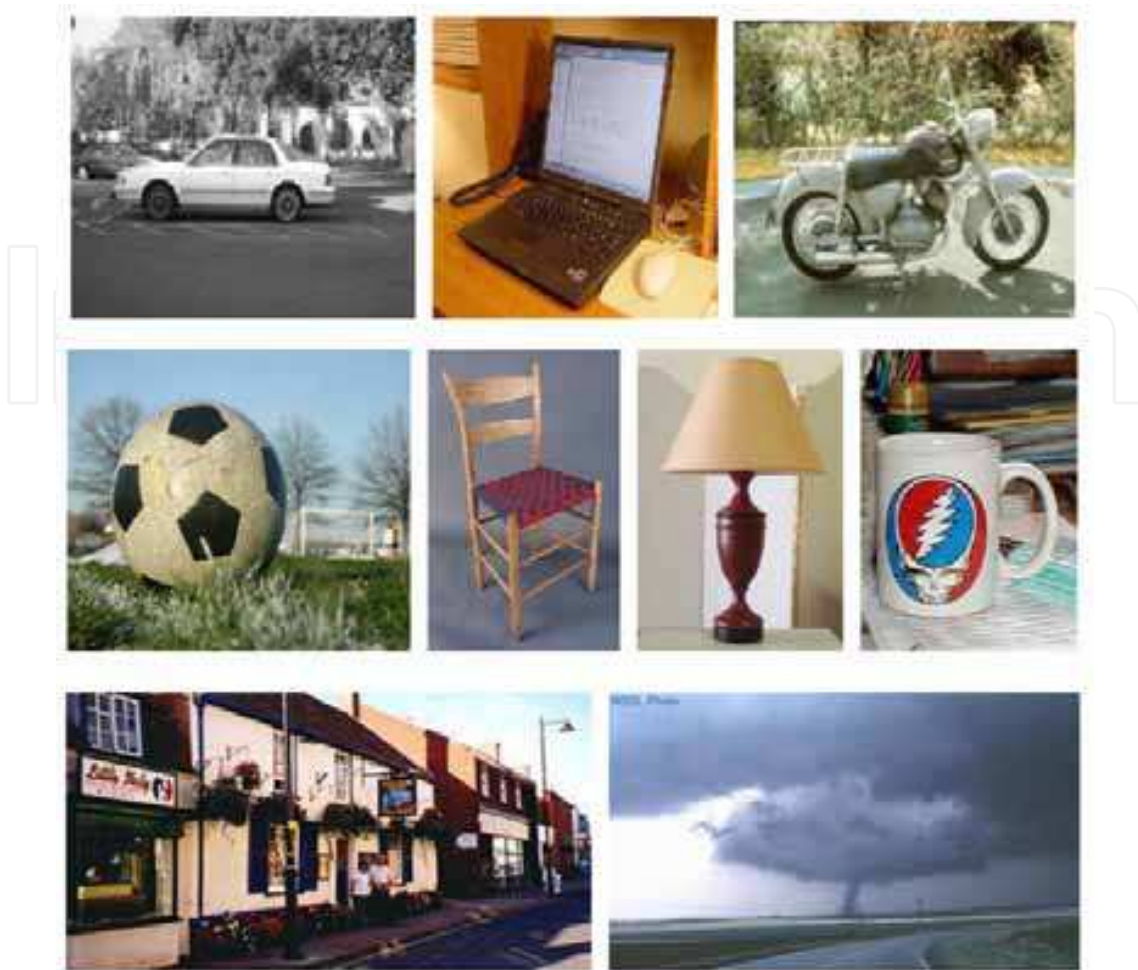


Fig. 11. Example images from CalTech101 database. The first and second rows show object, and the third row shows background

3.4.2 Object recognition after ego-motion compensation

The ego-motion of a humanoid robot causes the error of object recognition, the localization result changes according to the ego-motion, this generates errors. Ego-motion compensation system can cover this problem.

The notebook object from the real environment with ego-motion of UR1A can be recognized in the image sequence, and can be localized with a more accurate position after ego-motion compensation as shown in Fig. 25. The biggest three response patches are showed in Fig.25 in red boxes.

4. Conclusion

Humanoid robot should have the ability to recognize and localize generic object in real world image obtained from its vision system. A number of object recognition algorithms have been developed in computer vision, but there are some problems in the platform of humanoid robot because of the ego-motion. Therefore, this paper has the meaning of developing an ego-motion compensation method used for precise object recognition technologies for humanoid robot.

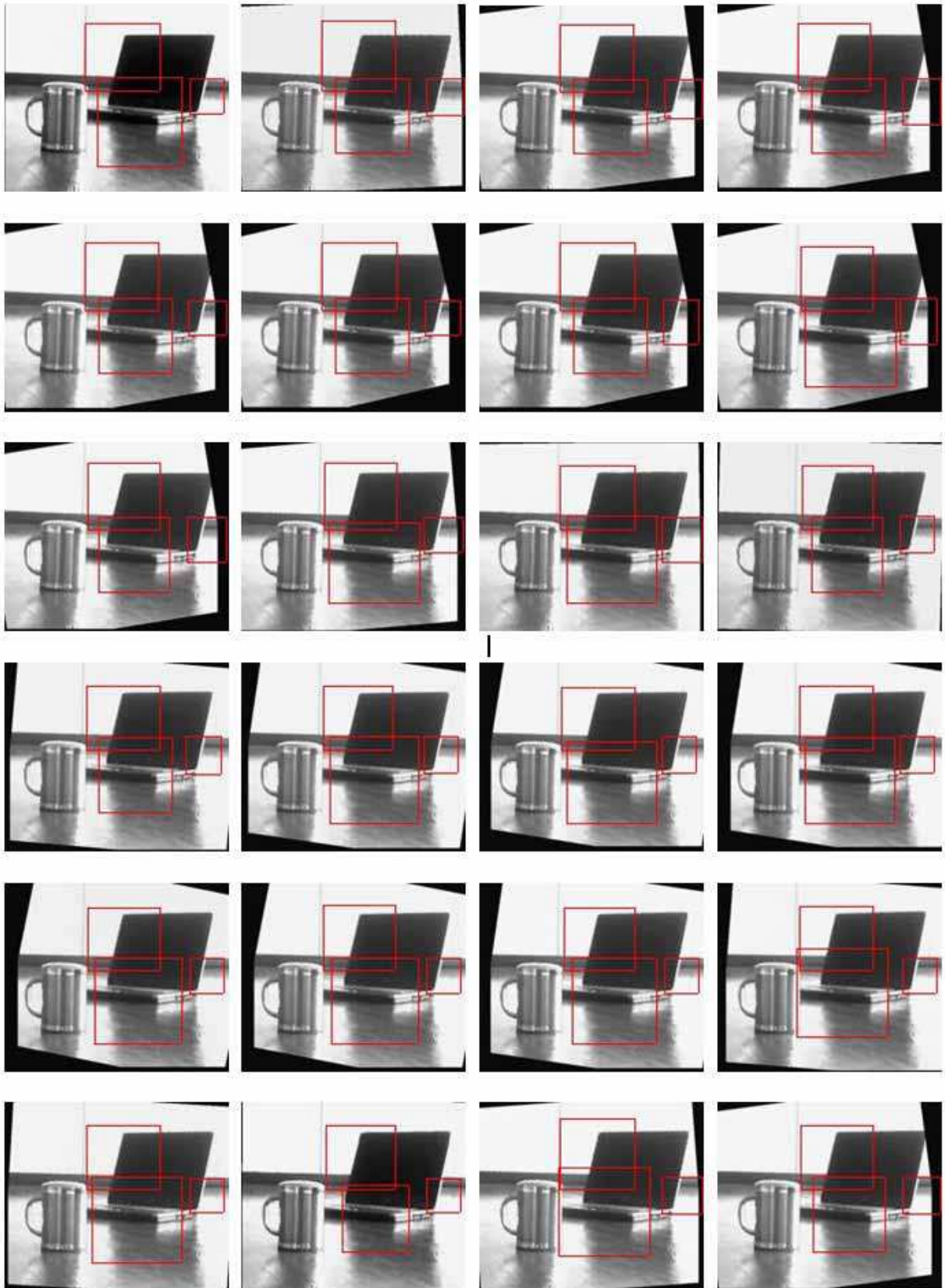


Fig. 12. Recognition result after ego-motion compensation. First row is the notebook image (left) and depth image (right) for real environment test.

A humanoid robot simultaneously shows the vertical and horizontal movement when it is walking, therefore, the ego-motion estimation method is proposed using stereo vision to cover this problem. Through the compensation of ego-motion, the image sequences are stabilized to improve the recognition accuracy, which means the transformations generated when a humanoid is working are eliminated.

The object recognition system is realized by SR4000 camera mounted in its head. Among several object recognition algorithms, improved HMAX model is used to category and localize the object. HMAX has been demonstrated to be an efficient model in computer vision, and is proved to be appropriate for generic object recognition for our humanoid robot platform.

In conclusion, the systems proposed in this paper are significantly useful in the sense that they are the characterized systems highly focused on and applicable to real-world humanoid robot.

5. Acknowledgments

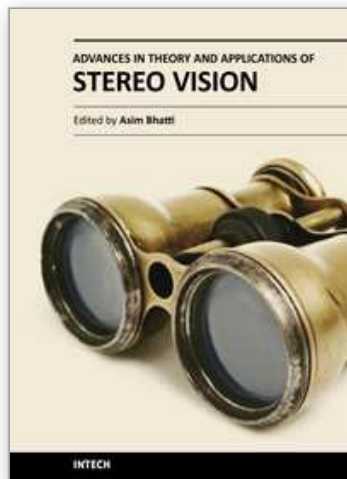
This work was supported by the Korean Institute of Construction & Transportation Technology Evaluation and Planning. (Program No.:06-United Advanced Construction Technology Program-D01)

6. References

- Hu R., Shi R., Shen I. and Chen W. (2007). Video Stabilization Using Scale-Invariant Features, *Proceedings of IV2007*, pp. 871-876.
- Milella, A., Siegwart R. (2006). Stereo-Based Ego-Motion Estimation Using Pixel Tracking and Iterative Closest Point, *Proceedings of International Conference on Computer Vision Systems*, pp.21-27.
- Lienhart R. and Maydt J. (2002). An Extended Set of Haar-like Features for Rapid Object Detection, *Proceedings of IEEE International Conference on Image Processing*, Vol. 1, pp.900-903.
- Beveridge J. R., She, K., Draper B. and Givens G. H. (2001). A nonparametric statistical comparison of principal component and linear discriminant subspaces for face recognition, *Proceedings of the IEEE Conference on Pattern Recognition and Machine Intelligence*, pp. 535-542, 2001.
- Morency L. P., Gupta R. (2003). Robust real-time egomotion from stereo images, *Proceedings of Intl. Conference on Image Processing*, Vol. 2, pp.719-722.
- Vedula S., Baker S., Rander P., Collins R. and Kanade T. (1999). Three-dimensional scene flow, *Proceedings of Intl. Conference on Computer Vision*, Vol. 2, pp.722-129, 1999.
- Mendel, (2001). *Uncertain Rule-Based Fuzzy Logic Systems: Introduction and New Directions*, Prentice-Hall.
- Hwang C., Rhee F. (2007). Uncertain Fuzzy Clustering: Interval Type-2 Fuzzy Approach to C-means, *IEEE Trans. on Fuzzy Systems*, vol.15 issue 1, pp. 107-120.
- Tizhoosh H. R. (2005). Image Thresholding using Type II Fuzzy Sets, *Pattern Recognition*, vol.38 pp. 2363-2372.

- Tizhoosh H. R. (2008) Type II Fuzzy Image Segmentation, *Fuzzy Sets and Their Extensions*, pp. 607-618.
- Tizhoosh H.R. (1998). On Thresholding and Potentials of Fuzzy Techniques, *Informatik'98*, Berlin, pp. 97-106.
- Mallat S. (1999). *A Wavelet Tour of Signal Processing*, Academic Press.
- Radim H., Jan F.(1998). Numerically Stable Direct Least Squares Fitting Ellipses, *Proceedings of Intl. Conf. on Computer Graphics and Visualization*, vol.1, pp. 125-132.
- Scharstein D. and Szeliski R., Middlebury Stereo Vision Page.
<http://vision.middlebury.edu/stereo/>.
- Caltech , Caltech 101 image database(2003).
<http://www.vision.caltech.edu/archive.html>

IntechOpen



Advances in Theory and Applications of Stereo Vision

Edited by Dr Asim Bhatti

ISBN 978-953-307-516-7

Hard cover, 352 pages

Publisher InTech

Published online 08, January, 2011

Published in print edition January, 2011

The book presents a wide range of innovative research ideas and current trends in stereo vision. The topics covered in this book encapsulate research trends from fundamental theoretical aspects of robust stereo correspondence estimation to the establishment of novel and robust algorithms as well as applications in a wide range of disciplines. Particularly interesting theoretical trends presented in this book involve the exploitation of the evolutionary approach, wavelets and multiwavelet theories, Markov random fields and fuzzy sets in addressing the correspondence estimation problem. Novel algorithms utilizing inspiration from biological systems (such as the silicon retina imager and fish eye) and nature (through the exploitation of the refractive index of liquids) make this book an interesting compilation of current research ideas.

How to reference

In order to correctly reference this scholarly work, feel free to copy and paste the following:

Tae-Koo Kang and Gwi-Tae Park (2011). Type-2 Fuzzy Sets Based Ego-Motion Compensation of a Humanoid Robot for Object Recognition, *Advances in Theory and Applications of Stereo Vision*, Dr Asim Bhatti (Ed.), ISBN: 978-953-307-516-7, InTech, Available from: <http://www.intechopen.com/books/advances-in-theory-and-applications-of-stereo-vision/type-2-fuzzy-sets-based-ego-motion-compensation-of-a-humanoid-robot-for-object-recognition>

INTECH
open science | open minds

InTech Europe

University Campus STeP Ri
Slavka Krautzeka 83/A
51000 Rijeka, Croatia
Phone: +385 (51) 770 447
Fax: +385 (51) 686 166
www.intechopen.com

InTech China

Unit 405, Office Block, Hotel Equatorial Shanghai
No.65, Yan An Road (West), Shanghai, 200040, China
中国上海市延安西路65号上海国际贵都大饭店办公楼405单元
Phone: +86-21-62489820
Fax: +86-21-62489821

© 2011 The Author(s). Licensee IntechOpen. This chapter is distributed under the terms of the [Creative Commons Attribution-NonCommercial-ShareAlike-3.0 License](#), which permits use, distribution and reproduction for non-commercial purposes, provided the original is properly cited and derivative works building on this content are distributed under the same license.

IntechOpen

IntechOpen